RSC Advances

Volume 1 | Number 1 | Jan 2013 | Pages 1–100

RSC Advances

www.rsc.org/advances

ROYAL SOCIETY OF CHEMISTRY

Suppressing phase coarsening in immiscible polymer blends by nano-silica particles located at the interface

Jian-Ming Feng, Xi-Qiang Liu, Rui-Ying Bao, Wei Yang, Bang-Hu Xie, Ming-Bo Yang*

College of Polymer Science and Engineering, Sichuan University, State Key Laboratory of
Polymer Materials Engineering, Chengdu, 610065, Sichuan, China

Abstract

The morphologies of polymer blends generated during processing are usually unstable and phase coarsening often occurs in the melt state, so suppressing the morphology coarsening is crucial to obtain polymer blends with tailored and stable structure and properties. The effect of nano-silica particles located at the interface on the phase coarsening of polypropylene (PP)/ polystyrene (PS) blend was studied in this work. In co-continuous 50/50 PP/PS blend, the particles at the interface can effectively suppress the coarsening process even at a very low particle loading. Real-time observation conducted by using an optical microscope equipped with a camera and a hot stage showed that a small loading of particles have little effect on the retraction process but can suppress the coalescence and at high loading of particles, both the retraction and coalescence process can be significantly suppressed. The suppressing effect towards the coalescence was confirmed in 70/30 blend with PS phase as the dispersed phase. The stabilization mechanism used in particle stabilized emulsions was adopted to explain the suppressing effect of nano-silica particles located at the interface towards the phase coarsening of PP/PS blends.

Keywords: Morphology coarsening; Particles; Coalescence; Suppression

---

* Corresponding author. Tel/Fax: + 86 28 8546 0130; *E-mail address:* weiyang@scu.edu.cn (W Yang)

1. Introduction

Phase coarsening is often observed in immiscible polymer blends when the blends are subjected to melt annealing or further melt processing owing to the large interfacial tension between components for immiscible polymer blends. During mixing, a large interfacial area is formed under shear and the generated phase morphologies are in non-equilibrium state. As a result, the phase morphologies start to change as soon as the melt of the blends leaves the mixer or the mixing section unless the melt are rapidly frozen. During further processing, if the blend is to be melted, the frozen-in phase morphology will start to change again and a huge increase of phase dimensions occurs usually, leading to the coarsening of phase morphologies of polymer blends. [1-9]

It has been reported that the interfacial tension is the driven force of phase coarsening and the coarsening can occurs via various patterns, viz. coalescence, and/or breakup, retraction and end-pinching,[10-17] which is intensely dependent on the blend composition and blend morphology. For the blends with initial droplet/matrix morphology, phase coarsening takes place via coalescence of droplets through which the interfacial area is reduced and hence the free energy of the system is minimized. Since the properties of polymer blends are highly dependent on phase morphologies, the unstable morphologies due to coarsening would eventually lead to unstable properties. So it is important and valuable to suppress the phase coarsening of polymer blends.

The most classical method to suppress phase coarsening is adding interfacial compatibilizers, often copolymers, into immiscible polymer blends, which can improve the interfacial interactions and effectively decrease the interfacial tension. Mekhilef,[18] Harrats,[19, 20] Yuan et al [21] reported that styrene–(hydrogenated butadiene)–styrene (SEBS) copolymer can effectively suppress the morphology coarsening of polystyrene (PS) /polyethylene (PE) blends. Omonov et al[22] found that the phase coarsening of reactively compatibilized co-continuous polypropylene (PP) / PS blends with PP-graft-PS was significantly retarded during thermal annealing.

Another potential method is the adoption of inorganic particles. In low viscosity liquid emulsions, a lot of studies have shown that inorganic particles can stabilize the emulsion morphology against coalescence.[23-28] Inspired by this, in our previous studies, we introduced nano-silica particles into PP/PS blends and studied the effect of the particles on the morphology coarsening.[29-30] Our studies showed that for polymer blends with co-continuous morphology and fibrous morphology, during melt annealing, the phase coarsening occurred via the retraction of the fibrous phases at first and the coalescence of the retracted droplets later. When nano-silica particles were selectively distributed in one phase, the relaxation of the molecular chains was inhibited which greatly suppresses the retraction process of this phase, and as a result, the overall phase coarsening of the blend morphology was suppressed. However, except that nano-particles totally distributed in only one phase in immiscible polymer blends, the particles may also selectively locate at the interface. In this study, we introduced the hydrophobic R974 nano-silica particles into PP/PS blends and studied the effect of their distribution at the interface on the morphology coarsening.

2. Experimental

2.1. Materials and sample preparation

The materials used were two commercial polymers: isotactic polypropylene (iPP, T30s, with a weight-average molecular weight of 387, 000 and a polydipersity of 3.6, Kunlun petrochemical co., LTD) and PS (PG-383M, Zhenjiang chimei chemical co., LTD). The nano-silica particles used, hydrophobic Aerosil R974, were purchased from Evonik Degussa Corporation, Germany. The particles have an average diameter of 12 nm and a hydroxyl density of 1.25 -CH_3/nm^2.

PP and PS were dried in a vacuum oven at 80 ^{o}C for 12 h before mixing. The melt compounding was conducted in a torque rheometer (XSS-300, Shanghai Kechuang Rubber Plastics Machinery Set Ltd., China) at 190 ^{o}C. During mixing, all the materials were added in the rheometer together and mixed at 50 rpm for 5 min. The content of filled nano-silica particles was 1, 2 and 4wt% relative to the mass of the whole blend.

2.2. Rheological tests

Rheological measurements were performed on a stress controlled dynamic rheometer (AR2000ex, TA Instruments, USA) equipped with 25mm parallel plate. Disk samples for rheological analysis were compression-molded at 190 ^{o}C and 10 MPa for 3 min. The thickness and diameter of samples were 2 and 25 mm, respectively. All the tests were carried out with a gap of 1.4 mm at 190 ^{o}C. Strain sweep was performed in the strain range of 0.1-100 % at 1Hz to determine the linear viscoelastic region of the samples, and the results showed that the linear viscoelastic region of all the samples was up to 20%. Dynamic frequency sweep was performed from 0.001 to 100 Hz within the linear viscoelastic regime. Stress relaxation tests were performed at a given strain of 20% to measure the shear stress $\sigma(t)$ as a function of time and the linear stress relaxation modulus G(t), which was obtained using $G(T) = \sigma(t)/\gamma_0$.

2.3. Morphology observation

Annealing treatment was carried out on a compression molding machine. The samples obtained by melt compounding were annealed for various periods of time at 190 °C and no pressure was applied during the annealing process. After annealing, the samples were quenched with cold water. The annealed samples were then cryo-fractured in liquid nitrogen. Contrast between the phases was achieved by immersing the samples in xylene for 6 h to selectively remove PS phase. The obtained samples were sputtered with gold to avoid charge accumulation and then observed at 20 kV using a scanning electron microscopy (SEM, JEOL JSM-5900LV, Japan).

Real-time monitoring of the coarsening process was conducted on an Olympus BX51 polarizing optical microscope (Olympus Co., Tokyo, Japan) equipped with a hot stage (LINKAM THMS 600). The sample films were compression-molded at a temperature of 190 °C and a pressure of 10 MPa. The films obtained were placed between two glasses fixed on the hot stage and quickly heated to 190 °C at a rate of 30 °C/min. After holding at 190 °C for 1 min, the gap between two glasses was decreased to 100μm. Then the morphology changing of the blends was recorded with a video camera.

3. Results and discussion

3.1 Distribution of nano-silica particles

Tab.1 Interfacial tension values of each pair in the blend at 23 and 190◦C

Possible pairs	Interfacial tension (mN/m)	
	23◦C	190◦C
PP/PS	1.4	2
PP/R974	2.1	1.8
PS/R974	2.	3.1

The distribution of R974 particles at equilibrium state can be predicated thermodynamically, as has been expounded elsewhere.[29] Here, the interfacial tension values of the PP/PS polymer blend and polymer/particle pair calculated by Wu's equation[31] are shown in Tab.1. Then the wetting coefficients (ω_1) at 23 and 190 ◦C can be calculated according to Sumita's theory. [32] The calculation shows that the wetting coefficient at 190◦C is 0.65 which indicates that the R974 particles will locate at the interface at thermodynamically equilibrium state at 190 ◦C.

Fig.1 shows the distribution of 2wt% R974 nano-silica particles in PP/PS blends with different composition. For 70/30 PP/PS blend in Fig.1a, R974 particles cover the surface of the dispersed PS phase. After extracting the PS phase, as shown in Fig.1b, the left particles are found to closely attach on the walls of PP phase, which is very different to hydrophilic A200 particles which fill the hole after the PS phase has been extracted [29], indicating that the R974 particles are located at the interface rather than in PS phase. In 50/50 PP/PS and 20/80 PP/PS blends, we can observe a similar distribution of R974 particles to that in 70/30 PP/PS blend. So we can confirm that the R974 particles prefer to locate at the interface at any blend composition, which accords well with the thermodynamic prediction.

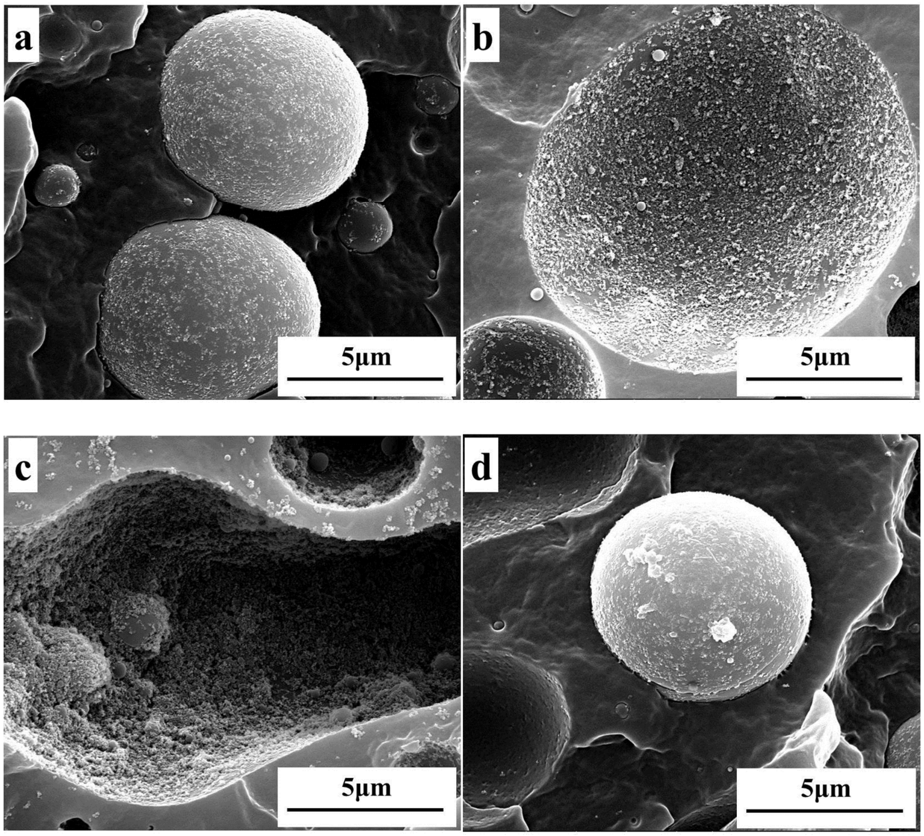

Fig.1 Morphology of 2 wt% R974 nano-silica particle filled PP/PS blends. (a,b)70/30 PP/PS blend; (c) 50/50 PP/PS blend; (d) 20/80 PP/PS blend, in which b and c are graphs with PS phase has been extracted by xylene.

3.2. Rheological behavior of PP/PS blends with particles at the interface

Melt rheology has been proved to be powerful to probe the dispersion of particles in polymer melt or the morphology of polymer blends, and the rheological responses of polymer blends are highly dependent on the components, compositions, phase morphology and interfacial interactions. When R974 nano-silica particles are selectively located at the interface, the interfacial interactions of PP and PS phase are changed, which can be reflected in the viscoelasticity of the blends. Fig. 2 shows the storage modulus (G'), loss modulus (G"), loss tangent (tanδ) and complex viscosity (η*) as a function of frequency for pure and R974 nano-silica particle filled 50/50 PP/PS blends at 190 ºC.

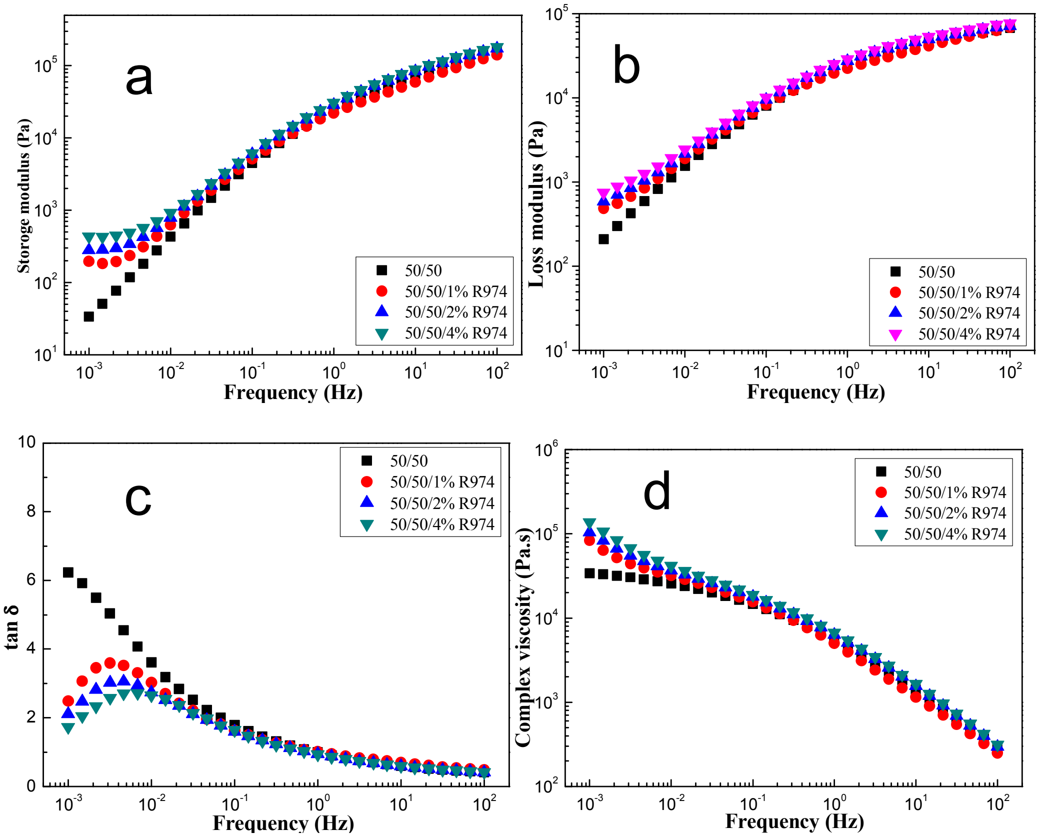

Fig.2 (a) Storage modulus, (b) loss modulus, (c) tan δ and (d) complex viscosity as a function of frequency for pure and hydrophobic nano-SiO_2 particle filled 50/50 PP/PS blends.

As we know, at low frequencies, polymer melt usually exhibits a characteristic terminal behavior with $G' \propto \omega^2$,[33-34] while for co-continuous blend, a characteristic terminal behavior of $G' \propto \omega$ is often found.[35] Here, pure 50/50 PP/PS blend performs a typical rheological behavior of co-continuous blend. However, when only 1wt% R974 particles are filled in the blend, the terminal behavior is significantly changed with a frequency independent modulus plateau present at low frequency regime. This is usually attributed to the formation of a hydrodynamically percolated particle network of the filled particles.[36-40] As has been shown, R974 particles selectively located at the interface of PP/PS blends regardless of the blend composition. For 50/50 PP/PS blend with co-continuous morphology, all the interface of the two phases are practically connected and form a channel throughout the blend. When the interfaces are occupied by particles, a particle network is naturally formed. According to Sumita,[41-42] the percolation threshold can be significantly reduced when particles are located at the interface. Fig. 3 shows the network structure formed by the R974 particles at the interface. It is found that the particles at the interface aggregate and form a tough shell covering the interface. With increasing loading of R974 particles, the particle network becomes more dense and tough, and the frequency independent plateau modulus increases (see Fig.2a).

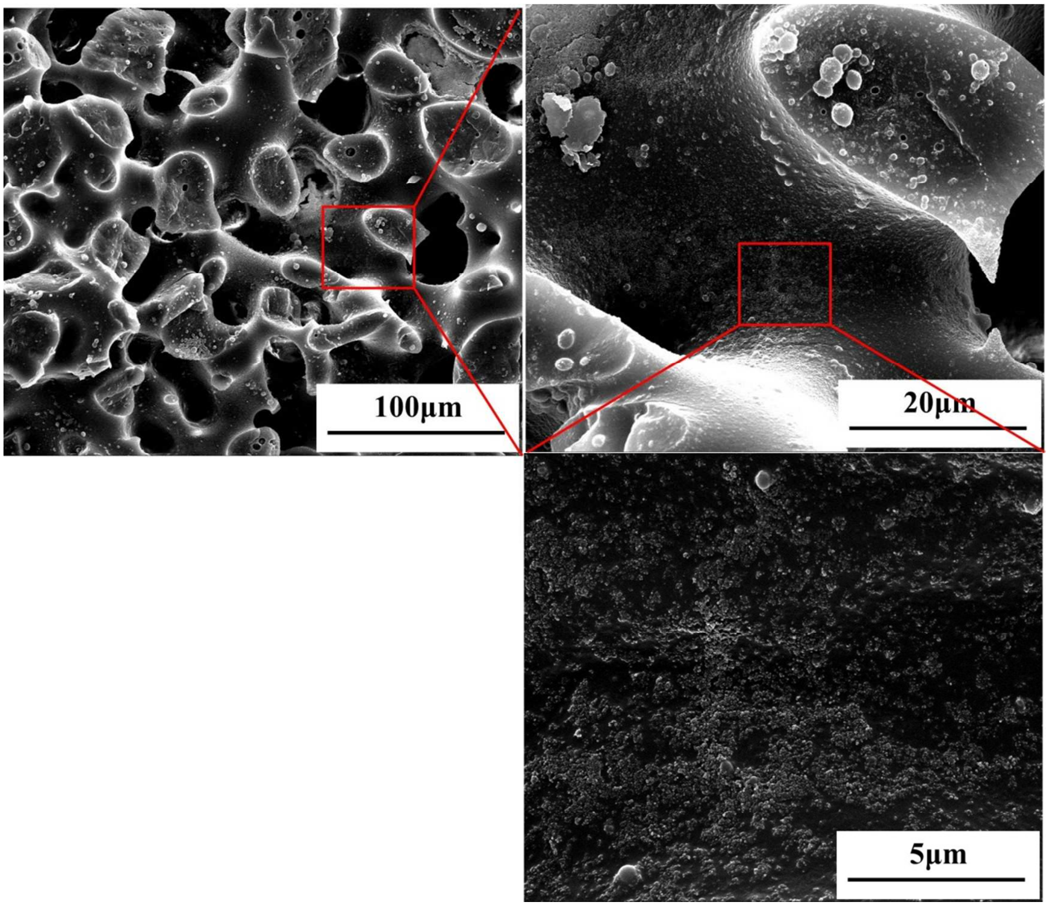

Fig.3 SEM micrographs of R974 particle network in 50/50 PP/PS blend with PS phase extracted.

3.3. Effects of nano-silica particles on the phase coarsening

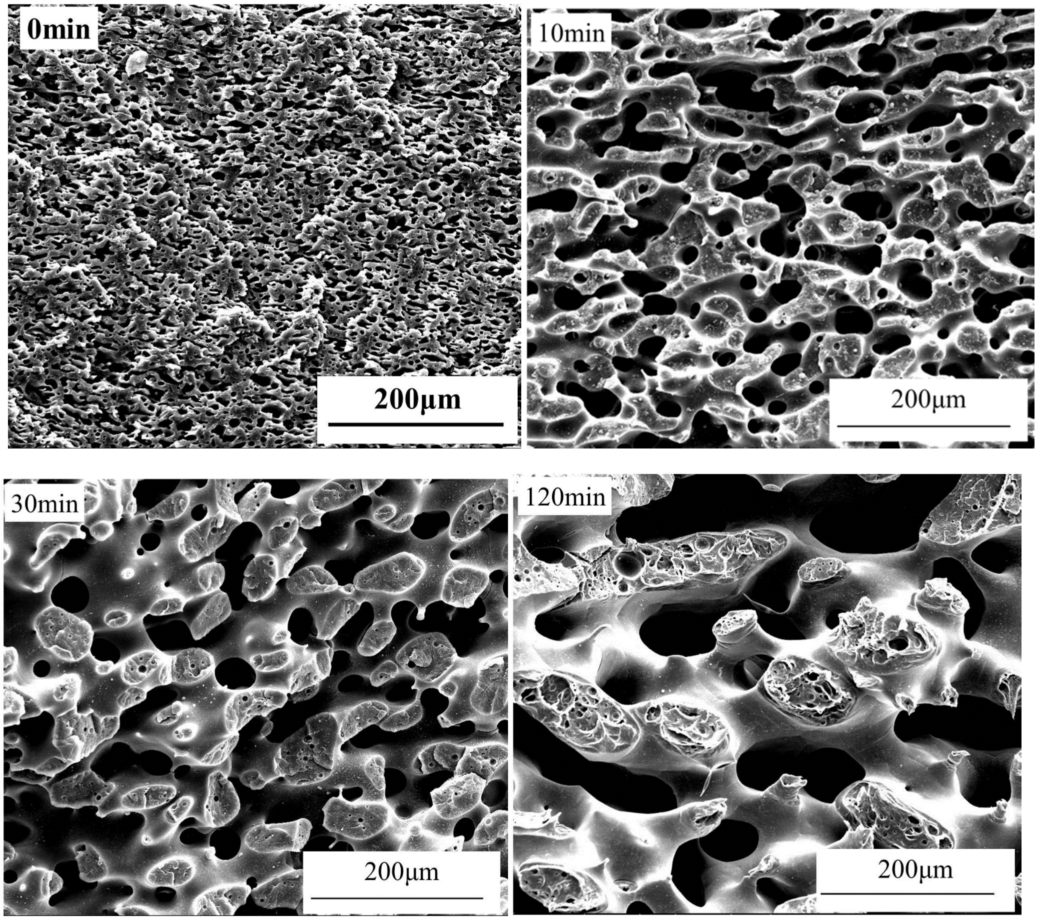

Fig.4 SEM micrographs of pure 50/50 PP/PS blend after annealing at 190 ºC for various time.

Fig. 4 and Fig. 5 show the morphology of 50/50 PP/PS blends filled with 0 and 1 wt% R974 nano-silica particles after annealing at 190 ^{o}C for various time, and more images can be seen in Fig. S1 in supporting information. The SEM micrographs show only PP phase after PS phase has been extracted by xylene. For all the blends, the initial co-continuous morphologies are preserved and both phases are continuous throughout the annealing process. This coarsening process has been reported for many 50/50 polymer blends. [43-45] However, upon annealing, the coarsening process differs very much for pure blend and the particle filled blends. The pure 50/50 blend shows a serve coarsening with the phase size increasing significantly while the 1wt% particle filled blend shows a slower coarsening process. According to the phase size statistics in Fig.6, the phase can grow from initial 6.7μm to 107.3μm after annealing for 2 hours for pure blend. When 1wt% R974 particles are introduced, after annealing for 2 hours, the phase size grows to 40μm, much smaller less than that of the pure blend. The coarsening process of 4wt% R974 particle filled blend was also evaluated and the phase size is only 22 μm after annealing 2 hours, indicating that the coarsening process can be significantly suppressed at higher particle concentration.

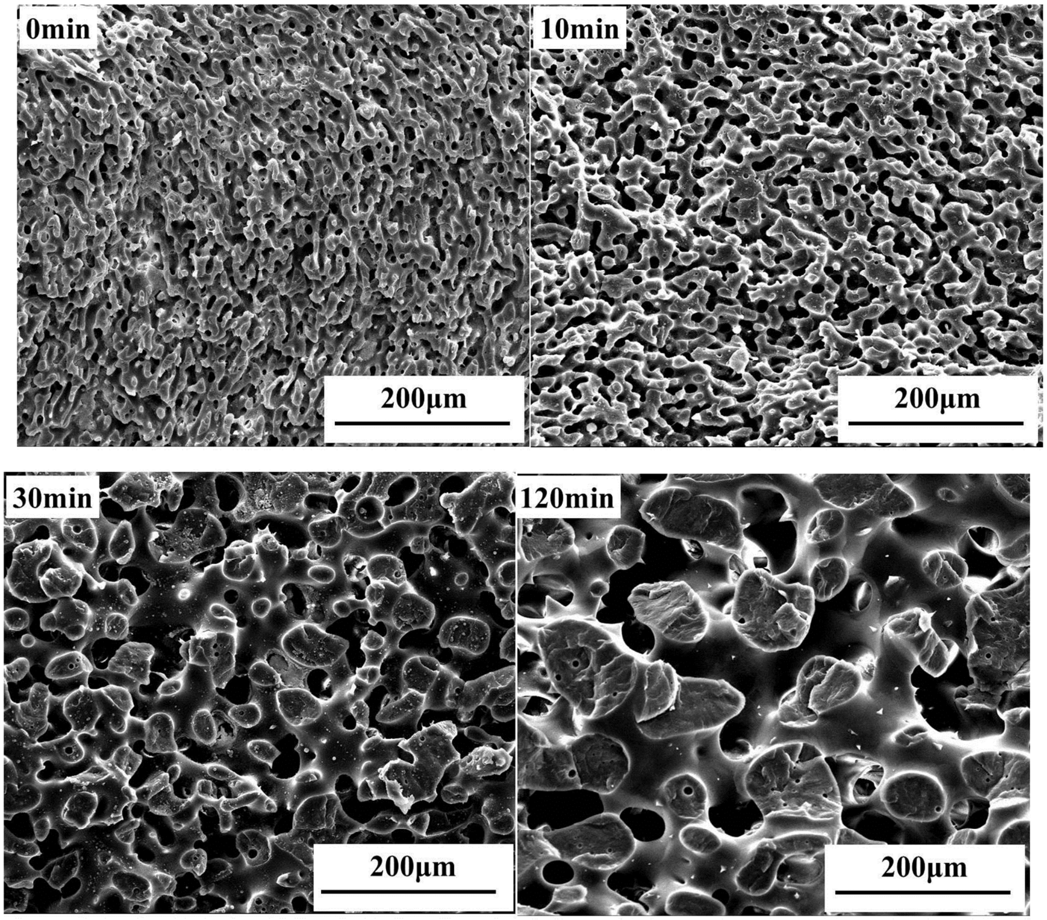

Fig.5 SEM micrographs of 1wt% R974 nano- SiO_2 particle filled 50/50 PP/PS blend after annealing at 190 ºC for various time.

From our previous study, the coarsening of co-continuous morphology can be divided into two stages which relate to two different coarsening mechanisms.[29] The first stage is mainly the retraction of elongated domains, this is a short process but with much higher coarsening rate, and the phase size can increase significantly in a short time. After that, the retraction becomes slow since most elongated domains have retracted, and then the blend morphology coarsens mainly by the coalescence of the retracted domains. The coarsening rate in the second stage is smaller but this process can last for a very long time, resulting that the phase size increases continuously for a very long time. From Fig.6, it is found that both stages are slowed down as can be seen from the decreased slopes of the curves after R974 particles are introduced. It can also be found that the suppression effect of the particles at the interface on the second-stage coarsening is stronger than the first-stage coarsening, especially in the blends filled with high content of particles. So the R974 particles located at the interface show a significant suppressing effect on the coalescence of the phases.

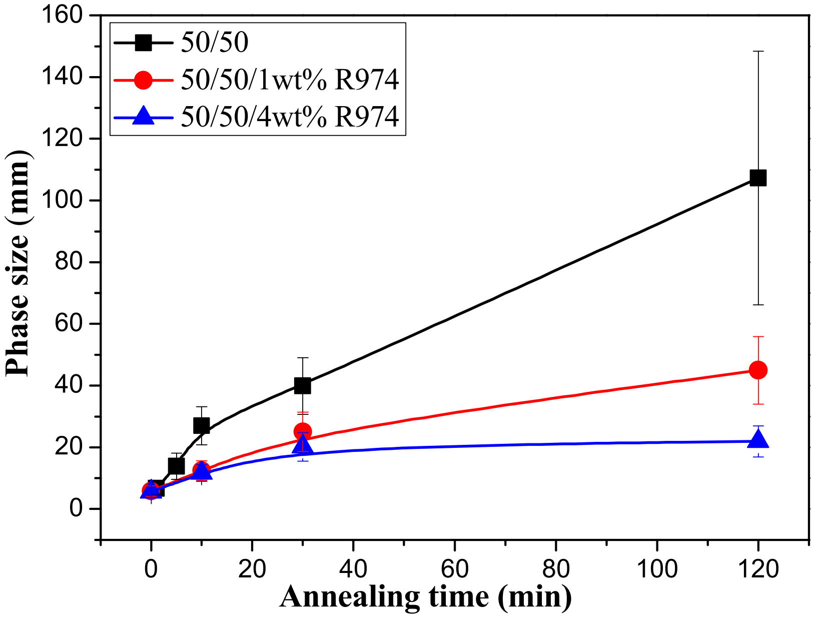

Fig.6 Phase sizes of pure and nano-SiO_2 particle filled 50/50 PP/PS blends after annealing at 190 ºC for various time.

3.4. Real-time monitoring of the coarsening process

To get a more direct view of the effect of R974 particles located at the interface on the coarsening process, we observed the coarsening process of pure and R974 particle filled blends in real time. Fig. 7 shows the real-time coarsening process of pure 50/50 PP/PS blends observed with an optical microscope during annealing at 190 ºC. In the beginning, the blend shows a co-continuous morphology with very small phase size. In a short time, the highly elongated domains retract into domains with smaller aspect ratios. After that, the retraction process becomes slow and less dominant. Coalescence is found throughout the coarsening process. But only when the elongated domains have retracted, the coalescence process becomes dominate. When 1wt% R974 particles are filled in the blends, as shown in Fig. 8, the elongated domains retract quickly in a short time, similar to that of pure blend. But after that, the coalescence of the retracted domains becomes slow. In a very long time, the size of the domains increases slowly with time, which is very different from that of pure blend. So a low content of R974 particles can effectively suppress the coalescence process even though the suppressing effect towards the retraction process is limited. We also observed the coarsening process of 4wt% particles filled 50/50 blend (shown in Fig. S2 in the supporting information) and found that during the 2 hour melt annealing, the phase size is less changed, indicating that both the retraction and the coalescence processes are significantly suppressed.

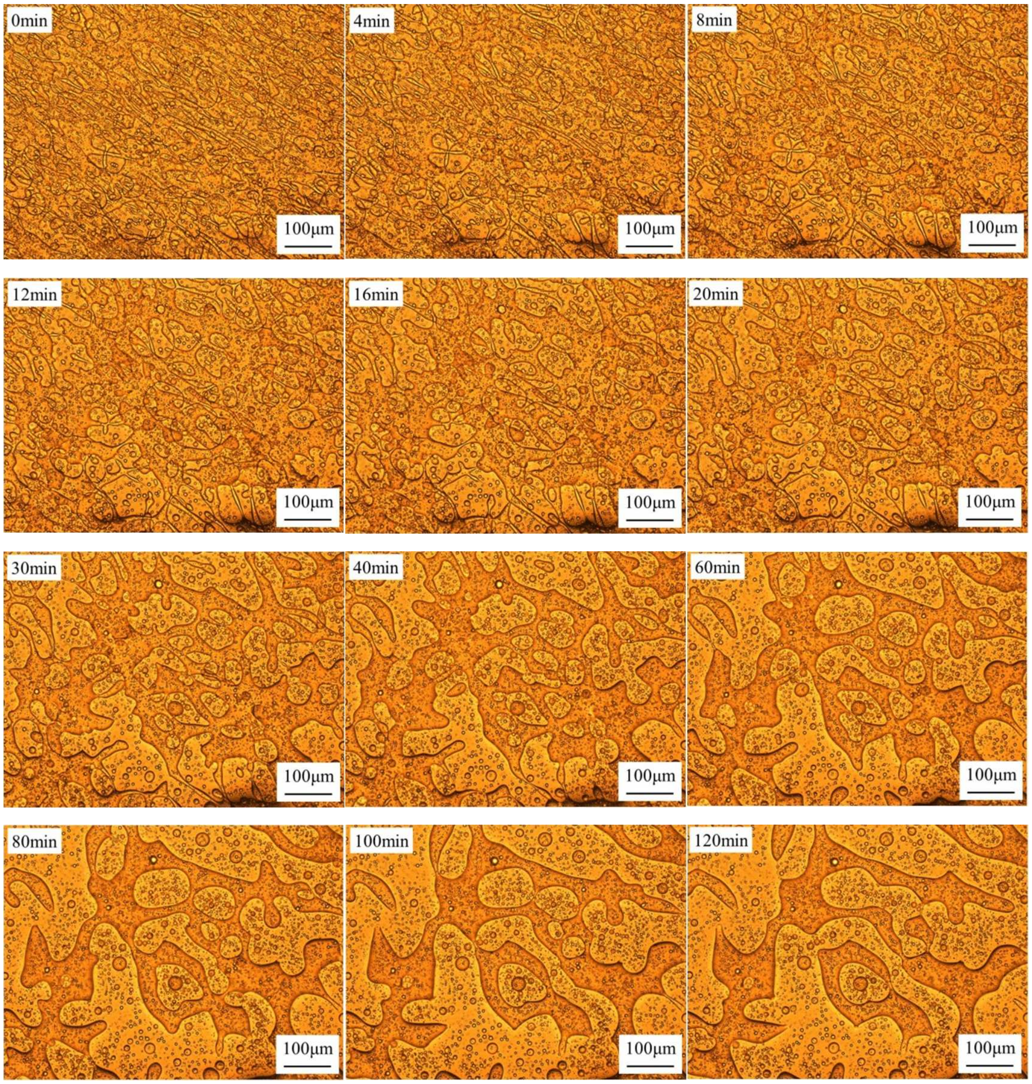

Fig. 7 Morphology evolution of pure 50/50 PP/PS blend observed by an optical microscope during annealing at 190 ºC.

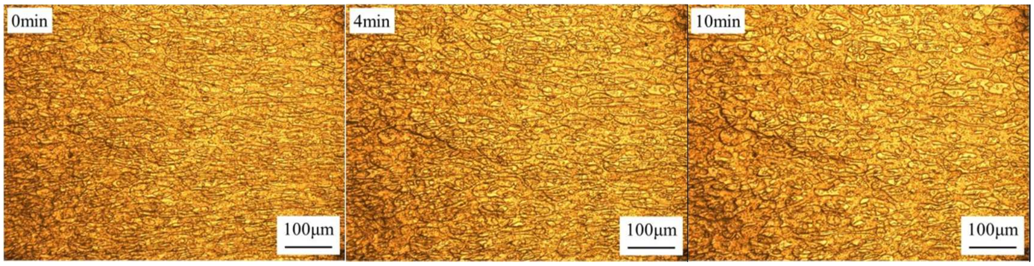

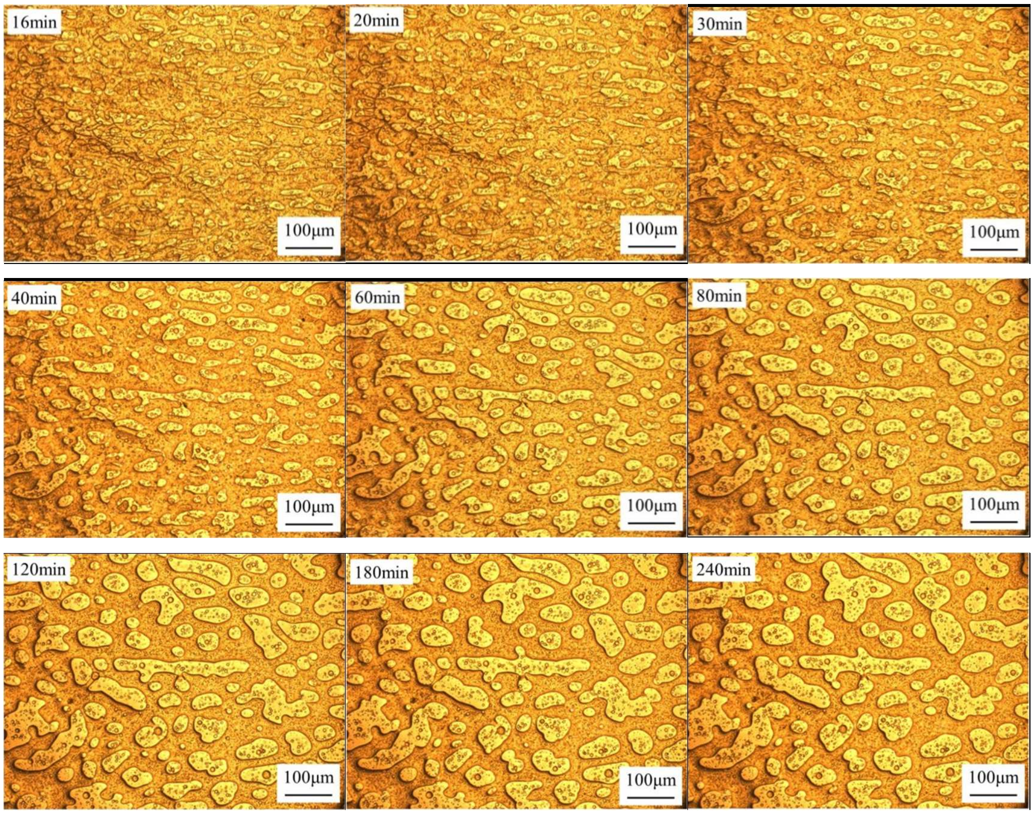

Fig. 8 Morphology evolution of 1wt% nano- SiO_2 particle filled 50/50 PP/PS blend observed by an optical microscope during annealing at 190 ºC.

To verify the suppression effect of the particles at the interface on the phase coalescence process, we also examined the blend with a composition of 70/30 (PP/PS) and observed the coalescence of PS droplets with and without R974 particles. It should be pointed out that at the blend composition of 70/30 (PP/PS), R974 particles at the interface cannot percolate in the blend since PS phase exists as droplets in PP matrix and the interface cannot form a connected channel as that in 50/50 (PP/PS) blend. R974 particles just cover the surface of PS droplets and form a tough particle shell, as shown in Fig.1b. Fig. 9 shows the morphology evolution of pure 70/30 PP/PS blend during annealing at 210 ºC. In the beginning, PS phase presents as highly elongated fibers. Then the PS fibers break up, retract, and finally become into spherical droplets. After 30min annealing, most PS fibers have become spherical droplets except for several fibers with a huge size. Then with annealing time increasing, coalescence of the droplets happens and the small spherical PS droplets collide, immerge and finally form much bigger spherical PS droplets. With only 1wt% R974 particle filled in the blend, as shown in Fig.10, the retraction of PS fibers is little affected, and most PS fibers can also retract in 30 min. After that, however, the retracted spherical PS droplets do not collide, immerge and form bigger spherical PS droplets as that in pure 70/30 blend. It seems like that ever since the retraction completes, the shape and the size of the droplets are fixed, indicating that further coalescence process is highly suppressed.

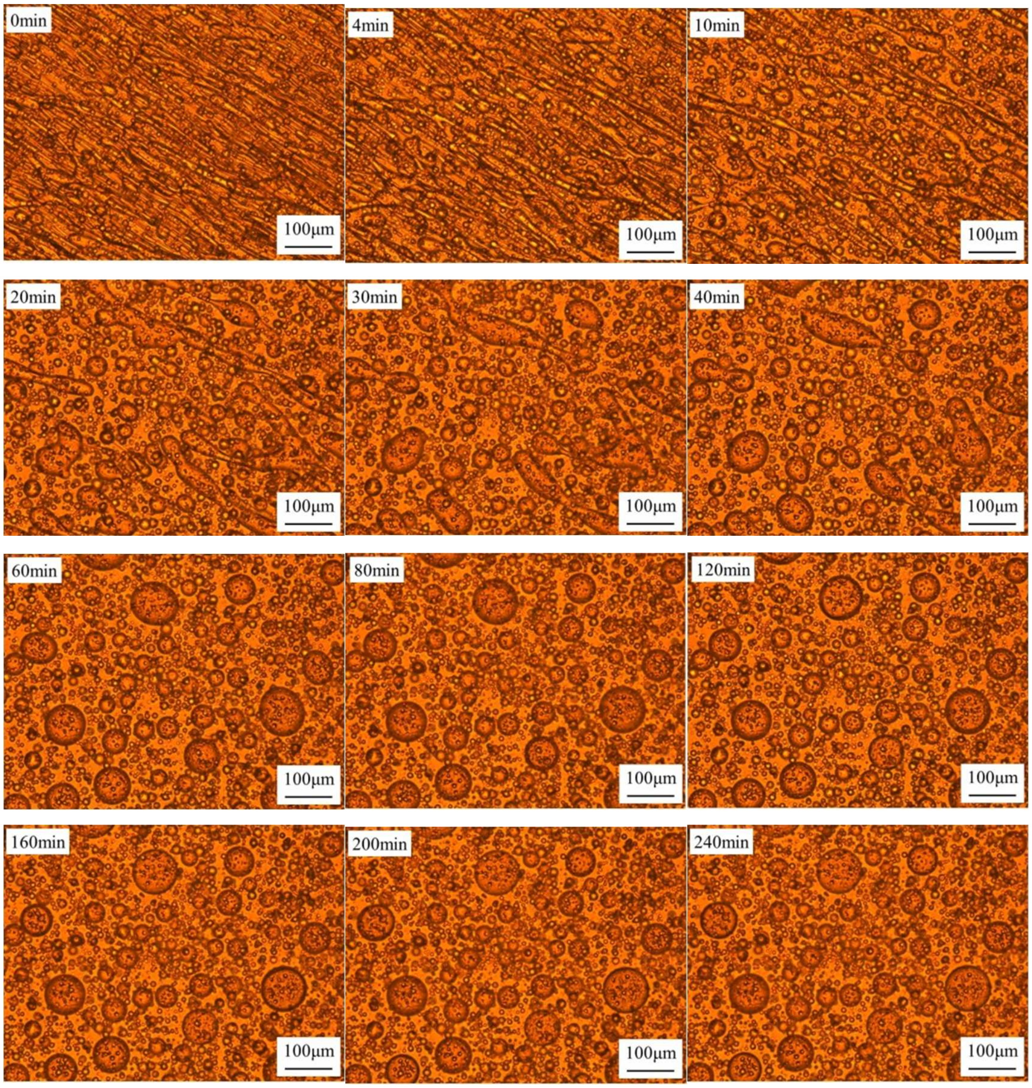

Fig. 9 Morphology evolution of 70/30 PP/PS blend observed by an optical microscope during annealing at 210 ºC.

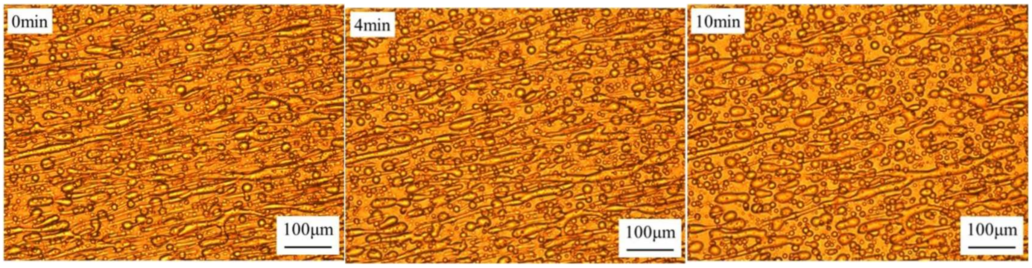

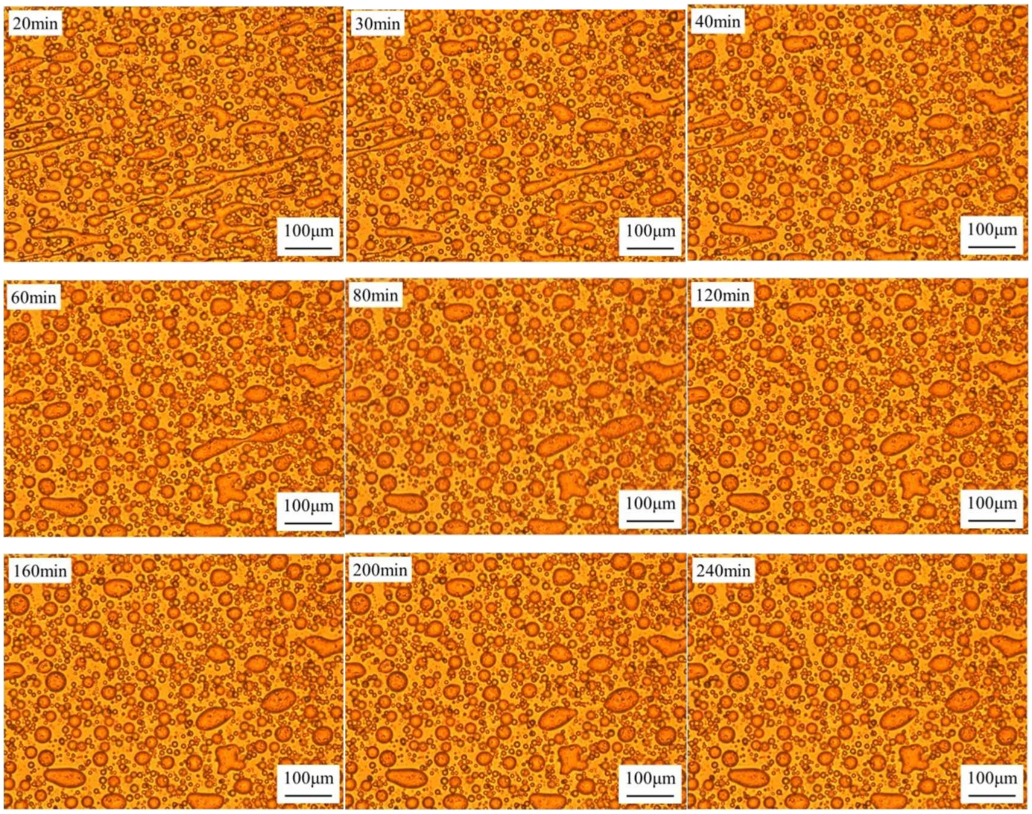

Fig.10 Morphology evolution of 1wt% nano- SiO_2 particle filled 70/30 PP/PS blend observed by an optical microscope during annealing at 210 ºC.

3.5. Discussion on the stabilization mechanism

Several models, such as Ostwald ripening and Brownian coagulation, have been proposed to describe the phase coarsening via coalescence of droplets. The theory of Ostwald ripening by Lifshitz and Slyozov[46] and Wagner[47] deals with the kinetics of the evaporation of molecules from small particles and condensation to large particles due to the curvature dependence of the chemical potential of different particles. The theory of Brownian coagulation by Binder and Stauffer[48] and Siggia[49] attributes the coarsening behavior to a collision between particles that is caused by the free thermal diffusion of particles without any interaction. Both mechanisms yield the same relation between the mean droplet radius R and the annealing time t:

$$\mathrm{R} = \mathrm{R}_0^3 + \kappa_\mathrm{i} \mathrm{t}$$

where R_0 is the initial radius at t_0, κ_i is a rate constant related to the coarsening mechanism.

Fortelný et al [50-54] proposed another coalescence mechanism in which they divided the coalescence course of dispersed droplets into four stages: (1) droplet approaching; (2) film draining (removal of the continuous phase between the droplets); (3) film rupturing and (4) the neck relaxing (evolution of the "neck" to form a coalesced droplet). They took the film-drainage time as the coalescence time between two droplets as the coalescence time between two droplets and arrived at different time dependencies of the mean droplet size by considering different interfacial mobility and driving forces. Following the work of Fortelný and Živný, Yu et al [55] also divided the coalescence process into four stages. They believed that the four stages have different impacts on coalescence. The first stage is mainly the result of Brownian motion, which makes more droplets collide and increases the touch probability of dispersed droplets. The remaining stages are the coalescence steps of two droplets, in which the time of rupture of the film is omitted because it is a relatively quick stage. Therefore, the total coalescence time, t, of two droplets can be written as the addition of the draining time of the film, τ_{drain}, and the merging time of the droplets,τ_{merge}:

$$\tau = \tau_{\mathrm{drain}} + \tau_{\mathrm{merge}}$$

About the stabilization of the phase morphology with the introduction of nano-SiO_2 particles located at the interface here, it is inevitable to mention the interfacial tension which is thought to be the driving force of phase coarsening. In emulsions stabilized by solid particles, it has been demonstrated by Okubo [56] and Vignati and Piazza [57] that the interfacial tension between the two liquids of the emulsion is unaffected by particle adsorption. However, Levine and Bowen [58] also pointed that due to the adsorption of particles at the interface, the area of the oil–water interface was reduced, which lowered the amount of energy required to form the interface. Therefore, a macroscopic or effective interfacial tension should be lower than that of the oil–water interfaces in the absence of particles.

Actually, the most reasonable stabilization mechanism unanimously recognized by which coalescence is inhibited is that the particle dense layers at the interface act as a mechanical barrier to prevent the drainage process. It has been established that the mobility of the interface is a critical parameter influencing the drainage process. Mobile interfacial layer allows faster film thinning while rigid interface slows down the process. [59-60] When R974 particles occupy the interface and cover the surface of PS droplets, the interface between PP and PS becomes rigid, so the drainage process will becomes much slower. So in R974 particle filled 70/30 PP/PS blend, in a very long time, neighboring droplets keep a distance and cannot approach to each other.

In addition, when film ruptures and the droplets merge, the particles must be removed from the droplet–droplet contact region and this can most likely be achieved by the lateral displacement of particles along the interface. [61] This is a slow process especially when the interactions between particles are strong and form a solid layer which renders the lateral displacement of particles more difficult. So for 1wt% R974 particle filled 50/50 PP/PS blend in which the two phases are separated by a layer of particles, the coalescence process can be slowed down. Certainly the coverage area of the particles plays an important role on the suppression effect. The partial coverage of the interface means that the droplets can coalesce after the particles in the contact region have been removed. If the interface has been completely covered by particles, the lateral displacement of particles becomes more difficult since there is no space for particles to move at the surface. This can also explain the significantly suppressed coalescence in 4wt% R974 particle filled 50/50 PP/PS blend. Actually, according to Tadros and Vincent [62] as well as Denkov et al [63], the particles can bridge the interfaces when two drops come into close proximity, forming a dense particle monolayer that prevents or retards a thin film of the second phase between the drops from draining.

4. Conclusions

In this work, we studied the effect of nano-silica particles located at the interface on the morphology coarsening of PP/PS blends. The adopted R974 nano-silica particles were found to selectively locate at the interface regardless of the blend composition and form a network structure at a small loading. SEM observations showed that with the formation of R974 particle network structure even at small loading of particles, the morphology coarsening process of co-continuous 50/50 blends can be suppressed when annealed in the melt state. By using real-time observation technique, it was found that the coalescence process was suppressed while the retraction process was little affected at a small loading of particles. Real-time observation of 70/30 PP/PS blend showed that the particles at the interface can suppress the coalescence process even though the particles cannot form a network structure in the blend. We adopted the stabilization mechanism used in particles stabilized emulsions to explain the suppressing effect of nano-silica particles towards the morphology coarsening of PP/PS blends. In 70/30 PP/PS blend, the drainage process was slowed down due to the rigid interface while in 50/50 PP/PS blend where both the two phases are continuous, the film rupture process was slowed down due to the coverage of particles.

Acknowledgements

The authors are grateful to the National Natural Science Foundation of China (Grant nos 21374065 and 51421061), the Major State Basic Research Development Program of China (973 program) (2012CB025902), the Innovation Team Program of Science & Technology Department of Sichuan Province (Grant 2014TD0002) and Sichuan Provincial Science Fund for Distinguished Young Scholars (2015JQO003). Mr Chao-liang Zhang, working at the State Key Laboratory of Oral Medicine of China, is also acknowledged for his kind help in FE-SEM observations.

References

1 J. J. Elmendorp and A. K. van der Vegt, Polym. Eng. Sci., 1986, 26, 1332–1338.

2 A. P. Plochocki, S. S. Dagli and R. D. Andrews. Polym Engng Sci, 1990, 30, 74.

3 T. Hashimoto, M. Takenaka, H. Jinnai, J. Appl. Crystallogr., 1991, 24, 457-466.

4 M. A. Huneault, Z. H. Shi and L. A. Utracki, Polym Engng Sci, 1995, 35, 115-127.

5 U. Sundararaj and C. W. Macosko, Macromolecules, 1995, 28, 2647–2657.

6 A. G. C. Machiels, K. F. J. Denys, J. Van Dam and A. Posthuma de Boe, Polym. Eng. Sci. , 1996, 36, 2451–2466.

7 R. C. Willemse, E. J. J. Ramaker, J. Van Dam and A. Posthuma de Boe, Polymer, 1999, 40, 6651–6659.

8 R. C. Willemse, E. J. J. Ramaker, J. Van Dam and A. Posthuma de Boe, Polym. Eng. Sci. , 1999, 39, 1717–1725.

9 Y. Y. Shi, W. B. Zhang, J. H. Yang, T. Huang, N. Zhang, Y. Wang, G. P. Yuan and C. L. Zhang, RSC Adv., 2013, 3, 26271–26282.

10 I. M. Lifshitz and V. V. Slyozov, J Phys Chem Solids 1961, 19, 35-50.

11 C. Z. Wagner, Elektrochemie, 1961, 65, 581-591.

12 I. Fortelný and A. Živný, Polymer, 1995, 36, 4113-4118.

13 I. Fortelný and J. Kovar, Polym. Compos., 1988, 9, 119-124.

14 I. Fortelný, Chem. Listy, 2013, 107, 791-797.

15 H. A. Stone, B. J. Bentley and L. G. Leal, J. Fluid Mech., 1986, 173, 131-158.

16 H. A. Stone and L. G. Leal, J. Fluid Mech., 1989, 198, 399-427.

17 W. C. Shi, W. Liu, J. Yang, Z. Y. He and C. C. Han, Soft Matter, 2014, 10, 2649–2655.

18 N. Mekhilef, B. D. Favis and P. J. Carreau, J. Polym. Sci., Part B: Polym. Phys., 1997, 35, 297-308.

19 C. Harrats, S. Blacher, R. Fayt, R. Jermˆoe and Ph. Teyssi´e, J. Polym. Sci., Part B: Polym. Phys., 1995, 33, 801-811.

20 C. Harrats, R. Fayt, R. Jermôe and S. Blacher, J. Polym. Sci., Part B: Polym. Phys., 2003, 41, 202-216.

21 Z. H. Yuan and B. D. Favis, J. Polym. Sci., Part B: Polym. Phys., 2006, 44, 711-721.

22 S. Tomotika, Proc. R. Soc. London, Ser. A, 1935, 150, 322–337.

23 W. Ramsden, Proc. R. Soc. London, Ser. A, 1903, 72, 156–164.

24 S. U. Pickering, J. Chem. Soc., Abstr. , 1908, 91–92, 2001–2021.

25 E. J. Stancik and G. G. Fuller, Langmuir, 2004, 20, 4805-4808.

26 D. A. Edwards, D. Brenner and D. T. Wasan, Interfacial transport processes and rheology. Butterworth-Heinemann, Boston, 1991.

27 D. E. Tambe and M. M. Sharma, Adv Colloid Interface Sci, 1994, 52, 1-63.

28 A. Van Blaaderen and A. Vrij, Langmuir, 1992, 8, 2921-2931.

29 X. Q. Liu, Q. Y. Wang, R. Y. Bao, W. Yang, B. H. Xie and M. B. Yang, RSC Adv., 2014, 4, 49429-49441.

30 X. Q. Liu, Z. Y. Sun, G. Q. Qi, R. Y. Bao, W. Yang, B. H. Xie and M. B. Yang, RSC Adv., 2014, 4, 41059-41068.

31 S. Wu, Polymer Interface and Adhesion, Marcel Dekker, New York, 1982, p. 534.

32 M. Sumita, K. Sakata, S. Asai, K. Miyasaka and H. Nakagawa, Polym. Bull., 1991, 25, 265-271.

33 D. S. Bangarusampath, H. Ruckdäschel, V. Altst¨adt, J. K. W. Sandler, D. Garray and M. S. P. Shaffer, Polymer, 2009, 50, 5803–5811.

34 R. V. Krishnamoorti, R. V. Vaia and G. P. Giannelis, Chem. Mater. , 1996, 8, 1728–1734.

35 D. Graebling, R. Muller, and J. F. Palierne, Macromolecules 1993,26, 320-329

36 C. A. Mitchell, J. L. Bahr, S. Arepalli, J. M. Tour and R. Krishnamoorti, Macromolecules, 2002, 35, 8825–8830.

37 C. A. Mitchell and R. Krishnamoorti, Macromolecules, 2007, 40, 1538–1545.

38 P. Pötschke, T. D. Fornes and D. R. Pau, Polymer, 2002, 43, 3247–3255.

39 Y. H. Song and Q. Zheng, Polymer, 2010, 51, 3262–3268.

40 N. Jouault, P. Vallat, F. Dalmas, S. Said, J. Jestin and F. Boué, Macromolecules, 2009, 42, 2031–2340.

41 M. Sumita, K. Sakata, S. Asai, K. Miyasaka and H. Nakagawa, Polym. Bull., 1991, 25, 265-271.

42 M. Sumita, K. Sakata, Y. Hayakawa, S. Asai, K. Miyasaka and M.Tanemura1, Colloid. Polym. Sc., 1992, 270, 134-139.

43 A. Pyun, J. R. Bell, K. H. Won, B. M. Weon, S. K. Seol, J. H. Je and C. W. Macosko, Macromolecules, 2007, 40, 2029–2035.

44 C. R. López-Barrón and C. W. Macosko, Langmuir, 2009, 25, 9392–9404.

45 C. R. López-Barrón and C. W. Macosko, Soft Matter, 2010, 6, 2637–2647

46 I.M. Lifshitz and V. V. Slyozov, J. Phys. Chem. Solids., 1961, 19, 35-50.

47 C. Z. Wagner, Elektrochemie, 1961, 65, 581-591.

48 K. Binder and D. Stauffer, Phys. Rev. Lett., 1974, 33, 17-21.

49 E. D. Siggia, Phys. Rev A., 1979, 20, 595-605.

50 I. Fortelný and A. Živný, Polymer, 1995, 36, 4113-4118.

51 I. Fortelný and J. Kovar, Polym. Compos., 1988, 9, 119-124.

52 I. Fortelný and A. Živný, Polymer 1998, 39, 2669-2675.

53 I. Fortelný, A. Živný and J. Juza, J. Polym. Sci. Part B., 1999, 37, 181-187.

54 I. Fortelný, Chem. Listy, 2013, 107, 791-797.

55 W. Yu, C. X. Zhou and I. Takashi, J. Polym. Sci. Part B., 2000, 38, 2378-2389.

56 T. Okubo, J. Colloid Interface Sci., 1995, 171, 55–62.

57 E. Vignati and P. Piazza, Langmuir, 2003, 19, 6650–6656.

58 S. Levine and B. D. Bowen, Colloid Surf. A., 1993, 70, 33-45.

59 E. J. Stancik. M. Kouhkan and G. G. Fuller, Langmuir 2004, 20, 90–94.

60 E. J. Stancik and G. G. Fuller, Langmuir 2004, 20, 805-808.

61 T. S. Horozov and B. P. Binks, Angew. Chem. Int. Ed., 2006, 45, 773-776.

62 Th. V. Tadros and B. Vincent, Encyclopedia of Emulsion Technology, Vol.1; Dekker: New York, 1983.

63 N. D. Denkov, I. B. Ivanov, P A. Kralchevsky and D. T. Wasan, J. Colloid Interface Sci., 1992, 150, 589-593.